PHYSICAL REVIEW D **84,** 055001 (2011)

LHC signatures of a vectorlike b'

S. Gopalakrishna,[1,*] T. Mandal,[1,†] S. Mitra,[2,‡] and R. Tibrewala[1,§]

[1]*Institute of Mathematical Sciences (IMSc), Chennai 600113, India*

[2]*Institute of Physics (IOP), Bhubaneswar 751005, India*

(Received 29 July 2011; published 1 September 2011)

Many beyond the standard model extensions predict the existence of heavy vectorlike fermions. We study the LHC signatures of one such heavy vectorlike fermion, called b', with electromagnetic charge $-1/3$ like the SM b-quark, but which could generically have different $SU(2)_L$ and $U(1)_Y$ quantum numbers. Our emphasis will be on the phenomenology due to $b \leftrightarrow b'$ mass mixing, present after electroweak symmetry breaking. We focus on aspects which distinguish a vectorlike b' from a chiral b' and include tree-level decays of the b' into tW, bZ and bh final states. While our analysis is largely model independent, we take as a motivating example warped-space models in which a vectorlike b' appears as the custodial partner of the top-quark.

DOI: 10.1103/PhysRevD.84.055001 PACS numbers: 12.60.Cn

I. INTRODUCTION

The standard model (SM) of particle physics suffers from the gauge hierarchy and flavor hierarchy problems and many extensions have been proposed to solve these problems. These theories beyond the standard model (BSM) predict extra particles that are being searched for at the CERN Large Hadron Collider (LHC). Among them are extra heavy fermions which could either be vectorlike or chiral. The purpose of this study is to analyze the LHC signatures of a vectorlike fermion which has electromagnetic charge $-1/3$, but depending on the model, can have various $SU(2)_L$ and $U(1)_Y$ quantum numbers. We refer to such a state as a b'. By vectorlike we mean that in the theory are present both a state in a representation of the gauge group and its conjugate representation, while a chiral state is one for which its conjugate representation is not present. A vectorlike fermion can have a bare mass consistent with gauge invariance, in contrast to a chiral fermion that obtains its mass due to the (spontaneous) breaking of the gauge symmetry.

The vectorlike nature of the b' can ascribe certain unique features to it which distinguishes it from a chiral b' that obtains its mass due to the SM Higgs vacuum expectation value (VEV). In the chiral case, the dominant decay mode of the b' is likely to be into tW, unless the $t'W$ is kinematically accessible (where the t' is a charge $2/3$ heavy fermion), induced by the charged current interaction. Also, in the chiral case, diagonalizing the mass matrix automatically diagonalizes the Higgs interactions, due to which a $b'bh$ coupling is absent at tree-level, while for a vectorlike theory, diagonalizing the mass matrix does not render the Higgs interactions diagonal due to the presence of the vectorlike mass term that is independent of the Higgs VEV. Thus, a vectorlike b' can have a tree-level $b' \to bh$ decay, which is not present at tree-level for chiral b' that gets its mass solely from the Higgs VEV. Furthermore, if the $SU(2)_L$ and $U(1)_Y$ quantum numbers of the b' are not the same as the b, generically, after electroweak symmetry breaking, an off-diagonal $b'bZ$ vertex is generated which allows the tree-level $b' \to bZ$ decay. Depending on the model, this branching ratio (BR) can be much bigger compared to a chiral b' that has identical $SU(2)_L$ and $U(1)$ quantum numbers as the b (for example, a fourth generation extension of the SM), for which this decay occurs only at loop level. At the LHC, largish $b' \to bZ$ and $b' \to bh$ BRs will reveal these aspects of the b'. In this work, therefore, we pay particular attention to the bZ and bh decay modes along with the tW decay mode, obtain b' cross sections for the significant production channels at the LHC, and analyze the reach for a vectorlike b'. We present our results quite model independently, but motivate our analysis in the context of warped-space models.

Chiral heavy fermions have been studied well in the literature, particularly in the context of fourth-generation models. Here we will study a vectorlike b' model independently, but keeping in mind, as an example, warped extra-dimensional theories [1] that have been proposed to solve the gauge-hierarchy problem. Because of the AdS/CFT correspondence conjecture [2], these are dual to four-dimensional strongly coupled theories. In variants of the original warped extradimensional proposal, the custodial partners of the top-quark (including the b') can be significantly lighter [3–6] than all the other Kaluza-Klein particles, making its observability at the LHC promising. Various studies have considered the LHC signatures of such TeV scale vectorlike fermions. Reference [7] considers the LHC signatures of a vectorlike b' by looking at 4-W events, along with signatures of a charge $5/3$ fermion, Ref. [8] considers the single and pair production of the

*shri@imsc.res.in
†tanumoy@imsc.res.in
‡smitra@iopb.res.in
§rtibs@imsc.res.in

charge $5/3$ custodial partner of the SM left-handed quark doublet exploiting same-sign dileptons to beat SM background, and the same-sign signal is also considered in Ref. [9]. Reference [10] studies pair production followed by decays into single and multilepton channels, and the pair production of the Kaluza-Klein top is explored in Ref. [11]. Signals due to mixing with light quarks and constraints have been analyzed in Ref. [12]. In Ref. [13] an exhaustive list of the single b' production processes at the LHC was given for the first time and new dominant processes were pointed out. This work draws heavily from the investigations there, which are being studied further [14]. For this model, the partial decay widths are worked out in Ref. [15]. On the experimental front, the Tevatron (CDF) bound is presented in Ref. [16] and is also discussed in Ref. [17]. Recent LHC (CMS) bounds from the $b' \to tW$ decay mode is presented in Ref. [18]. Our emphasis here will be to include b' single and pair production, and, $b' \to bZ$ and $b' \to bh$ decay modes in addition to $b' \to tW$, and keeping it model independent. Single production depends more directly on the electroweak quantum numbers of the b', while b' pair production is dominated by its coupling to the gluon (which is given by the $SU(3)_C$ gauge coupling g_S) and thus hides its electroweak nature. For this reason, in addition to pair production, we will consider single production also in our work.

The paper is organized as follows: In Sec. II we present the effective Lagrangian in a model-independent way showing the coupling of the b' to SM fields, and identify the relevant parameters for our work. In Sec. III we derive expressions for the b' partial decay widths. In Sec. IV we explore the $b'\bar{b}'$ pair production and $b'Z$, $b'h$ single production, particularly focussing on bZ and bh decays going into the semileptonic and dileptonic final states, compute signal and background cross sections with appropriate cuts, and compute the luminosity required at the 14 TeV LHC for 5σ significance with at least 10 events. For the semileptonic mode, we include the dominant QCD background, in addition to the irreducible electroweak background. We present these results model independently by varying the relevant couplings and the b' mass. We list a few other b' single-production processes very briefly and mention the reasons why we do not consider them in detail. In Sec. V we offer our conclusions.

II. b' MASS MIXING AND COUPLINGS

We consider an extension of the SM with a heavy (TeV scale) vectorlike b'. Generically, after electroweak symmetry breaking, the SM b mixes with the b' due to off-diagonal terms in the mass matrix. After taking into account this mixing, we can go from the (b, b') basis to the (b_1, b_2) mass basis and write the Lagrangian model independently in the mass basis as

$$\begin{aligned}\mathcal{L}_{4D} \supset & -\frac{e}{3}\bar{b}_1\gamma^\mu b_1 A_\mu - \frac{e}{3}\bar{b}_2\gamma^\mu b_2 A_\mu \\ & + g_s\bar{b}_1\gamma^\mu T^\alpha b_1 g_\mu^\alpha + g_s\bar{b}_2\gamma^\mu T^\alpha b_2 g_\mu^\alpha \\ & - (\kappa^L_{btW}\bar{t}_L\gamma^\mu b_{1L}W^+_\mu + \kappa^L_{b_2tW}\bar{t}_{1L}\gamma^\mu b_{2L}W^+_\mu + \text{H.c.}) \\ & + \kappa^L_{bbZ}\bar{b}_{1L}\gamma^\mu b_{1L}Z_\mu + \kappa^L_{b_2b_2Z}\bar{b}_{2L}\gamma^\mu b_{2L}Z_\mu \\ & + (\kappa^L_{b_2bZ}\bar{b}_{1L}\gamma^\mu b_{2L}Z_\mu + \text{H.c.}) \\ & + \kappa^R_{bbZ}\bar{b}_{1R}\gamma^\mu b_{1R}Z_\mu + \kappa^R_{b_2b_2Z}\bar{b}_{2R}\gamma^\mu b_{2R}Z_\mu, \end{aligned} \tag{1}$$

and the Higgs interactions as

$$\begin{aligned}\mathcal{L}_{4D} \supset & -\frac{h}{\sqrt{2}}[\kappa_{hb_Lb_R}\bar{b}_{1L}b_{1R} + \kappa_{hb_{2L}b_{2R}}\bar{b}_{2L}b_{2R} \\ & + \kappa_{hb_Lb_{2R}}\bar{b}_{1L}b_{2R} + \kappa_{hb_{2L}b_R}\bar{b}_{2L}b_{1R}] + \text{H.c.}. \end{aligned} \tag{2}$$

We omit a few other possible terms in Eq. (1) for the following reasons: our interest will be in theories in which the mass mixing is between $b_L \leftrightarrow b'_L$ without b_R mixing, which is the reason why we do not introduce $\kappa^R_{b_2bZ}\bar{b}_{2R}\gamma^\mu b_{1R}Z_\mu + \text{H.c.}$. Also, we will assume that the $W_L \leftrightarrow W_R$ mixing is small (where the W_R is the $SU(2)_R$ gauge boson if this symmetry is gauged), and that the b' is a singlet under $SU(2)_L$, which is why we do not include a $\kappa^R_{b_2tW}\bar{t}_{1R}\gamma^\mu b_{2R}W^+_\mu + \text{H.c.}$ term. For convenience, in the text, we use (b, b') interchangeably with the mass eigenstates (b_1, b_2), but in our numerical work we distinguish them properly.

Here we consider a single b' for simplicity, but in general, there could be more than one b' that mixes with the b, and our work can be straightforwardly extended to models with more than one b'.[1]

Here, we present the phenomenology in a model-independent manner, and vary the mass of the b' (denoted as M_{b_2}) in presenting the phenomenology. We stipulate that the underlying BSM model must ensure that $\kappa^{L,R}_{bbZ}$, κ_{btW} and $\kappa_{hb_Lb_R}$, to a good approximation, take their respective SM values to be consistent with experimental data. In the BSM extensions we are interested in, $\kappa_{hb_{2L}b_R}$ will be very small and therefore we set this to zero in our analysis. We take the remaining κ's, namely, $\kappa^L_{b_2bZ}$, κ_{b_2tW}, $\kappa_{hb_Lb_{2R}}$, $\kappa^{L,R}_{b_2b_2Z}$, and $\kappa_{hb_{2L}b_{2R}}$ as free parameters; our phenomenology will only depend on the first three of these κ's, and the

[1]Unless the $SU(2)_L \otimes U(1)_Y$ quantum numbers of the b' are the same as that of the b, mixing to a single b' puts a stringent lower bound on the b' mass ($M_{b'} \gtrsim 3$ TeV) from the requirement that the shifts to the $Zb\bar{b}$ coupling be smaller than the constraint from precision electroweak data. For example, in the warped-space model in Ref. [13] with the b mixing to a single b' with *different* $SU(2)_L \otimes U(1)_Y$ quantum numbers, we explicitly see that the $Zb\bar{b}$ coupling gets shifted. This can be avoided by either ensuring that the $SU(2)_L \otimes U(1)_Y$ quantum numbers of the b' is the same as that of the b, or, by mixing to more than one b'. The latter is the case for instance for the warped-space model in Ref. [19].

TABLE I. The benchmark masses and couplings used in this study. These are obtained for the warped model in Ref. [13].

M_{b_2} (GeV)	250	500	750	1000	1250	1500
$\kappa^L_{b_2bZ}$	0.185	0.121	0.084	0.064	0.051	0.043
κ_{b_2tW}	0.322	0.161	0.107	0.080	0.064	0.054
$\kappa_{hb_Lb_{2R}}$	0.714	0.937	0.972	0.985	0.990	0.993
M_{b_2} (GeV)	1750	2000	2250	2500	2750	3000
$\kappa^L_{b_2bZ}$	0.037	0.032	0.029	0.026	0.024	0.022
κ_{b_2tW}	0.046	0.040	0.036	0.032	0.029	0.027
$\kappa_{hb_Lb_{2R}}$	0.995	0.996	0.997	0.998	0.998	0.998

last two are largely irrelevant here. This is because although the b' pair production has contributions due to the last two couplings, they are subdominant compared to the gluon exchange channel, and, the last two couplings are not relevant for single production or decay of the b'.

We analyze the phenomenology in the following sections for the benchmark masses and couplings shown in Table I. These are the couplings obtained for the warped-space model considered in Ref. [13] where the κ_{ijk} are explicitly worked out for the $b' \subset (1, 2)$ representation of $SU(2)_L \otimes SU(2)_R$.

III. b' DECAY

The heavy mass eigenstate b_2, once produced, decays via the off-diagonal interaction terms in Eqs. (1) and (2). Thus, the main decay modes are $b_2 \to b_1 Z$, $b_2 \to b_1 h$ and $b_2 \to tW$, and these tree-level decays are shown in Fig. 1. As already mentioned, the presence of the $b_1 h$ decay mode uniquely signals the vectorlike nature of the b'. The partial widths into these decay channels are

$$\Gamma_{bZ} = \frac{(\kappa^L_{b_2bZ})^2}{32\pi} M_{b_2} \cdot \left(\frac{1}{x_Z^2} + 1 - 2x_{bZ}^2 + x_b^2 - 2x_Z^2 + x_{bZ}^2 x_b^2\right) \times (1 + x_Z^4 + x_b^4 - 2x_Z^2 - 2x_b^2 - 2x_Z^2 x_b^2)^{1/2}, \quad (3)$$

$$\Gamma_{tW} = \frac{(\kappa^L_{b_2tW})^2}{32\pi} M_{b_2} \cdot \left(\frac{1}{x_W^2} + 1 - 2x_{tW}^2 + x_t^2 - 2x_W^2 + x_{tW}^2 x_t^2\right) \times (1 + x_W^4 + x_t^4 - 2x_W^2 - 2x_t^2 - 2x_W^2 x_t^2)^{1/2}, \quad (4)$$

$$\Gamma_{bh} = \frac{M_{b_2}}{64\pi}\left[(\kappa^2_{hb_{2L}b_R} + \kappa^2_{hb_Lb_{2R}})\left(1 - x_h^2 - \frac{3}{4}x_b + x_b^2\right) + \frac{5}{2}\kappa_{hb_{2L}b_R}\kappa_{hb_Lb_{2R}}x_b\right] \times (1 + x_h^4 + x_b^4 - 2x_h^2 - 2x_b^2 - 2x_h^2 x_b^2)^{1/2}, \quad (5)$$

where $x_i = m_i/M_{b_2}$, $x_{ij} = m_i/m_j$, and, Γ_{bZ}, Γ_{tW} and Γ_{bh} denote the partial widths of the b' to the bZ, tW and bh final states, respectively.

Since the b_2bh coupling in Table I is large, Γ_{bh} can be sizable. The Γ_{bZ} dependence on $1/x_Z^2$ due to the longitudinal polarization of the Z_μ enhances this partial width for large M_{b_2} and can make it comparable to Γ_{bh}. The same holds also for the Γ_{tW}.

We show in Fig. 2 the partial widths of the b' to the bZ, tW and bh final states, in a model-independent fashion, in the $\kappa - M_{b_2}$ plane. The blue dots show the relation between the M_{b_2} and κ as shown in Table I, and the partial widths in this model can be read off from the plots.

IV. LHC SIGNATURES

At a hadron collider such as the LHC, the production can proceed through the gg, gq and qq initial states, where instead of q we can have a b-quark too. For sub-TeV b' mass, we expect the g parton distribution function (pdf) to be bigger than the q and b pdf, and therefore we expect the gg, gq and qq signal (and background) rates to be in decreasing order. Therefore, to get good significance, if

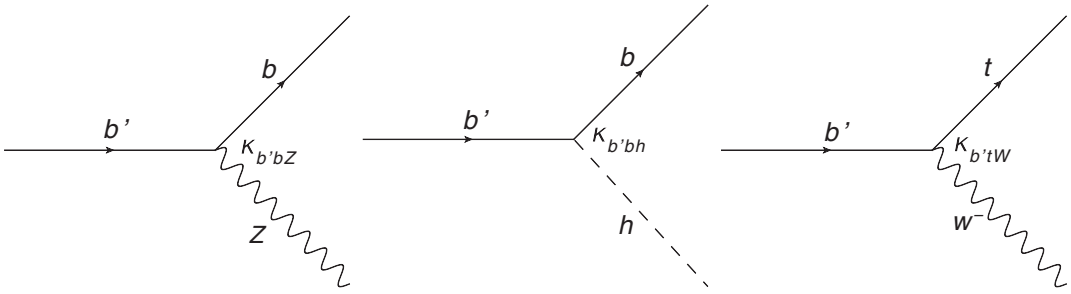

FIG. 1. The tree-level decay modes of the b'.

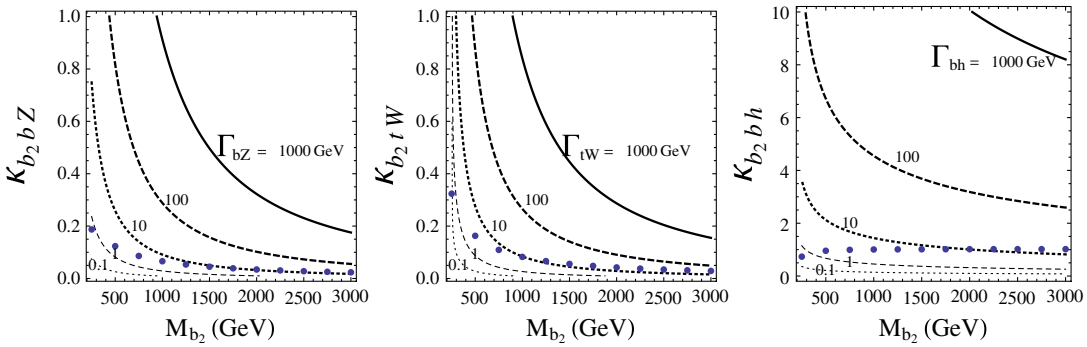

FIG. 2 (color online). Contours of partial widths of the b' to the bZ, tW and bh final states. The blue dots show the relation between the M_{b_2} and κ as shown in Table I.

the signal is qq initiated, for example, the background should not be gg or gq initiated, and similarly for the other possibilities. If the b' is not too heavy, the $gg \to b_2 b_2$ pair production is expected to have the largest production rate compared to single production owing to the larger gluon pdf. But the QCD background will also be large. For processes for which QCD induced background is not present, the single-production channel can lead to a good reach at the LHC. Single production of the b' proceeds via the off-diagonal couplings in Eqs. (1) and (2).

In this study, we consider $pp \to b'\bar{b}'$, $b'Z$ and $b'h$ processes as the discovery channel of the b' and to show its vectorlike character. We compute the signal cross section for various masses and compute the main irreducible SM backgrounds for these channels using Monte Carlo event generators. We have defined the warped-space model with the vectorlike b' in the matrix-element and event generators MADGRAPH 5 Version 1.3.2 [20] and CALCHEP Version 2.5.6 [21], and all our results in this section are obtained using these event generators. We use CTEQ6 [22] parton distribution functions.

In order to make the multiparticle phase-space Monte Carlo integration tractable timewise, wherever possible, we use the narrow-width approximation and multiply by the appropriate branching ratios in order to obtain the required cross section in the channel considered. This will mean that the acceptance in transverse momentum (p_T) and rapidity (y) for the final state particles will not be taken into account exactly, but since we mostly deal with high p_T particles, the inaccuracies should be small. These agree very well as the p_T of the Z becomes large, and we find, for instance, the agreement to be better than 10% for $M_{b'} \gtrsim 500$ GeV.

In the following, we analyze b' production at the LHC followed by the $b' \to bZ$, tW, or bh decay modes. As mentioned in Sec. I, this will help in revealing the vectorlike nature of the b'. We devise kinematic cuts to establish signal events above SM background, and obtain the luminosity required for the benchmark points in Table I at the 14 TeV LHC to obtain at least 5σ statistical significance and for observing at least 10 events.

To obtain model-independent results, we use the cross sections for the benchmark points in Table I and factor out the known dependence on the couplings κ and $M_{b'}$ to make a fit to the purely kinematical part of the cross section (including the pdf and phase-space factors). Once this fit is made, we fold back in the dependence on the couplings and mass and obtain the cross section for any value of these parameters model independently, and infer the required luminosity.[2]

A. $pp \to b'\bar{b}'$ process

In this section we analyze the b' pair production which is initiated by the gg initial state as shown in Fig. 3. Since the production cross section is mostly dominated by the b' coupling to the gluon (with gauge coupling constant g_S), our results for the production are largely model independent.[3] In Fig. 4 (left) we show the $pp \to b'\bar{b}'$ cross section in fb as a function of M_{b_2} after p_T and y cuts. These cuts are applied after the bZ decay of both the b', requiring $-2.5 < y_{b,Z} < 2.5$ and $p_{Tb,Z} > 25$ GeV as we detail next.

1. $b'\bar{b}' \to bZ\bar{b}Z$ decay mode

We consider here both the b's decaying into the bZ final state resulting in the $bZ\bar{b}Z$ final state. We demand two tagged bs, consider the semileptonic channel taking one of the Zs to decay hadronically (including only u, d, c;s, but not the b) and the other Z decaying leptonically ($\ell = e$ and μ with $\mathrm{BR}(Z \to \ell\ell) = 0.066$), resulting in the channel $pp \to b'\bar{b}' \to bZ\bar{b}Z \to bl^+l^-\bar{b}jj$. To avoid having to deal with combinatorics issues with the four bs that will be present if the Z decays to $b\bar{b}$, we ask that this not happen by demanding that the tagged-b is not among the two jets that reconstruct to the Z. We obtain the signal and electroweak background cross section at the $bZbZ$ level and

[2]For a model-independent study in the extended minimal supersymmetric standard model context, see Ref. [23].

[3]We have roughly estimated the effective ggh (top triangle diagram) contribution to $b'\bar{b}'$ production and find this to be much smaller than the gluon exchange contribution.

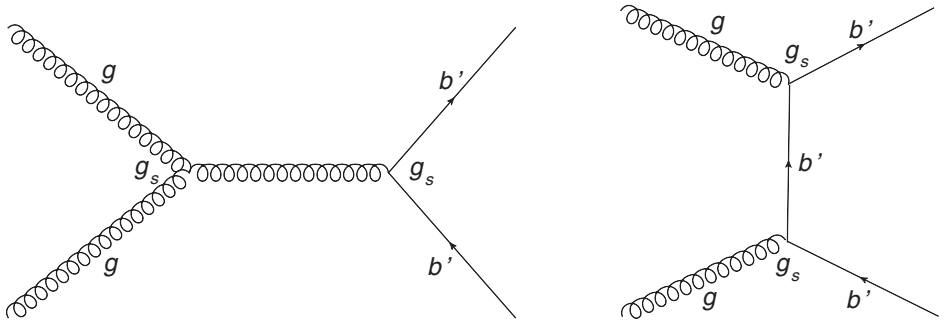

FIG. 3. The partonic Feynman graphs for $pp \to b'\bar{b}'$ at the LHC. We show only the gg initiated graphs as examples.

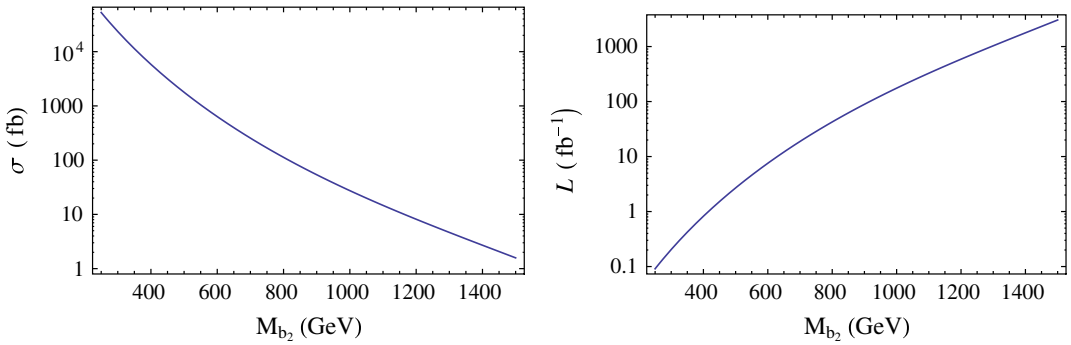

FIG. 4 (color online). $pp \to b'b'$ cross section after p_T and y cuts (left), and, the luminosity required for 5σ significance with at least 10 signal events in the $pp \to b'\bar{b}' \to bZ\bar{b}Z \to b\ell\ell\bar{b}jj$ channel after all cuts (right), with $\mathrm{BR}(b' \to bZ) = 1/3$ assumed. These are for the 14 TeV LHC.

multiply the $\sigma(pp \to bZbZ)$ cross section by the factor $2\eta_b^2 \mathrm{BR}_{Z\to\ell\ell}(\mathrm{BR}_{Z\to jj} + \mathrm{BR}_{Z\to bb}(1-\eta_b)^2) = 0.019$ with $j = \{u, d, c, s\}$, where, η_b is the b-tagging efficiency, the $\mathrm{BR}_{Z\to bb}$ term counts the $Z \to b\bar{b}$ decays that fail the b-tag, and a factor of 2 is because the hadronic-Z and the leptonic-Z can be exchanged resulting in the same final state. We take the b-tagging efficiency $\eta_b = 0.5$. We obtain the QCD background at the $bjjbZ$ level as we explain in more detail below.

To maximize the signal at the expense of the SM background, we apply the following cuts: *Rapidity*: $-2.5 < y_{b,j,Z} < 2.5$, *Transverse momentum*: $p_{Tb,j,Z} > 25$ GeV, *Invariant-mass cuts*: $M_Z - 10\ \mathrm{GeV} < M_{jj} < M_Z + 10\ \mathrm{GeV}$, $0.95M_{b_2} < M_{(bZ)} < 1.05M_{b_2}$. where, in the last invariant-mass cut, we accept the event if the invariant mass of a b with either Z lies within the invariant-mass window, *and*, the invariant mass of the other b with either Z also lies within the window.

We show in Table II the signal and background cross sections after y, p_T and invariant-mass cuts as a function of $M_{b'}$ with the corresponding κ as shown in Table I, and show the luminosity required at the 14 TeV LHC for 5σ significance with the requirement that at least 10 signal events be observed. The $(bjjbZ)_{\mathrm{tot}}$ column in Table II shows the total background which is the sum of the QCD and electroweak backgrounds, where the QCD background is got from the components shown in the second table as

$$(bjjbZ)_{\mathrm{QCD}} = (bjjbZ) + (1-\eta_b)(bbjbZ) + (1-\eta_b)^2(bbbbZ),$$

where b includes both b and $\bar{b}$, and the $(1-\eta_b)$ factors take into account a b-quark that has failed the b-tag, i.e. we assume here that a b-quark that fails the b-tag will be taken to be a light-jet. We find that the luminosity required is signal-rate limited.

The results shown here are largely model independent since the production cross section mostly relies on the color quantum number of the b' since the cross section is dominated by the gluon exchange contribution, with a coupling of g_s. In Fig. 4 (right) we show the luminosity required for 5σ significance with at least 10 signal events at the 14 TeV LHC, in the $pp \to b'b' \to bZbZ \to b\ell\ell bjj$ channel after all cuts, with $\mathrm{BR}(b' \to bZ) = 1/3$ assumed.

The dileptonic mode, i.e. when both Zs decay leptonically, is much cleaner since there is no QCD background, but the BR is smaller. Since we are limited by signal rate, we expect the luminosity required to be much bigger than for the semileptonic mode we have focussed on. The luminosity required for the dileptonic mode can easily be computed from the signal and $bZbZ$ background cross sections given in Table II after taking into account the

TABLE II. Signal and background cross sections at the 14 TeV LHC for the process $pp \to b'\bar{b}' \to bZ\bar{b}Z$, and the luminosity required ($\mathcal{L}$) in the semileptonic decay mode, for the benchmark masses and couplings shown in Table I. The $bZbZ$ columns do not include b-tagging factors, BR($Z \to \ell\ell$) or BR($Z \to jj$), while $\mathcal{L}$ includes all these factors. $(bjjbZ)_{\rm tot}$ shows the total background (including electroweak and QCD) where the QCD background is computed using the channels detailed in the second table weighted by appropriate factors as explained in the text.

M_{b_2} (GeV)	Signal σ_s (in fb) $bZbZ$		Background σ_b (in fb) $bZbZ$		$(bjjbZ)_{\rm tot}$		$\mathcal{L}$ (fb^{-1})
	y, p_T cuts	All cuts	y, p_T cuts	All cuts	y, p_T cuts	All cuts	
250	25 253	25082	21.804	0.3797	16 938	29.52	0.021
500	171.34	148.69	21.804	0.047	16 938	3.74	3.514
750	14.508	12.221	21.804	0.0097	16 938	0.997	42.752
1000	2.314	1.9214	21.804	0.0027	16 938	0.259	271.92
1250	0.484	0.399	21.804	0.0011	16 938	0.048	1310

M_{b_2} (GeV)	QCD background (in fb) $bjjbZ$		$bbjbZ$		$bbbbZ$	
	y, p_T cuts	All cuts	y, p_T cuts	All cuts	y, p_T cuts	All cuts
250	16790	27.304	255.41	2.7	81.01	1.92
500	16790	3.513	255.41	0.256	81.01	0.194
750	16790	0.958	255.41	0.031	81.01	0.057
1000	16790	0.2514	255.41	0.0052	81.01	0.008

$\mathrm{BR}_{Z\to\ell\ell}$ for the other Z also. One can also consider demanding only one b-tag rather than the two that we have, which will increase the signal rate, but so will the background, although the luminosity required may end up being lesser.

2. $b'\bar{b}' \to bZ\bar{b}h$ and other decay modes

We only consider a light Higgs decaying as $h \to b\bar{b}$ (with BR ≈ 1), i.e. the $b'\bar{b}' \to bZ\bar{b}h \to bZ\bar{b}b\bar{b}$ channel, and demand four b-tags. For this, the σ multiplied by the branching fractions and b-tagging efficiency, shown earlier, will be about half the $bZbZ$ case shown in Table II and in Fig. 4 (left). The dominant SM backgrounds will then be $bbbbZ$, which we have already computed for the previous case and shown in Table II. As we can see from this, for large $M_{b'}$, the required luminosity will be signal-rate limited as it was in the previous case, and therefore the luminosity required will be about twice that needed for the $bZbZ$ case shown in Table II and in Fig. 4 (right).

One could also consider the $bZtW$ or other combinations of decay modes of the b' pair, but we do not consider these here, as our main motivation is to focus on those decay modes which help in revealing aspects of the vectorlike nature of the b'.

B. $pp \to b'Z$, $b'h$ processes

In this section, we analyze the $pp \to b'Z$ and $pp \to b'h$ processes which are initiated by the bg initial state as shown in Fig. 5. In Fig. 6 (left) we show contours of the $pp \to b'Z$ cross section in fb, after p_T and y cuts, in the $\kappa^L_{b_2bZ} - M_{b_2}$ plane at the 14 TeV LHC. These cuts are applied after the $b' \to bZ$ decay, requiring $-2.5 < y_{b,Z} < 2.5$ and $p_{Tb,Z} > 0.1 M_{b_2}$. The blue dots show the $M_{b'}$ and $\kappa^L_{b_2bZ}$ as given in Table I.

The $b'h$ cross section is expected to be similar to the $bg \to b'Z$ case above. In the following, we consider the $b' \to bZ$, tW or bh decay modes. For the bZh final state both $bg \to b'h \to bZh$, and $bg \to b'Z \to bhZ$ channels

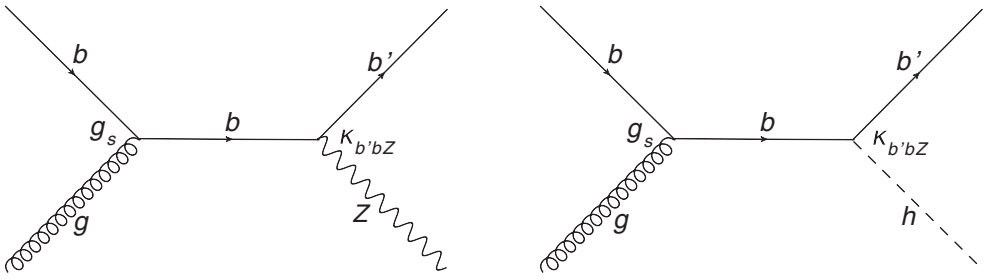

FIG. 5. The partonic Feynman graphs for $pp \to b'Z$, $b'h$ at the LHC.

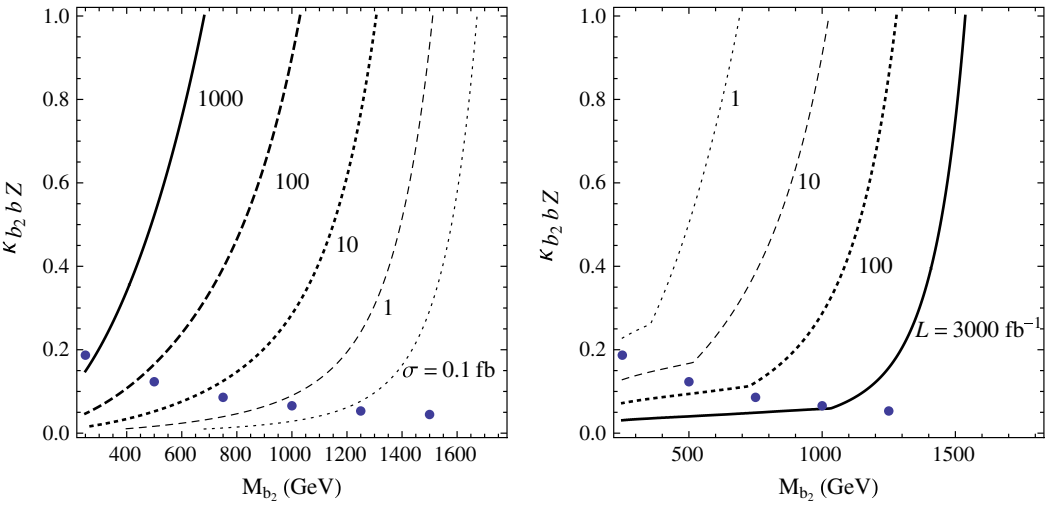

FIG. 6 (color online). Model-independent contours of the $pp \to b'Z$ cross section in fb after p_T and y cuts (left), and, contours of the luminosity required for 5σ significance with at least 10 signal events in the $pp \to b'Z \to bZZ \to b\ell\ell jj$ channel after all cuts (right), with the region to the left of a contour covered by that luminosity, and $\mathrm{BR}(b' \to bZ) = 1/3$ assumed. These are for the 14 TeV LHC. The blue dots show the $M_{b'}$ and $\kappa_{b_2 bZ}$ as given in Table I.

will contribute. We will discuss each of these channels, in turn, next.

1. $bg \to b'Z \to bZZ$ channel

We will consider next, in turn, the semileptonic decay mode when one Z decays leptonically and the other hadronically (i.e. $bZZ \to bjj\ell^+\ell^-$), and, dileptonic decay mode when both Zs decay leptonically (i.e. $bZZ \to b\ell^+\ell^-\ell^+\ell^-$).

Semileptonic decay mode: For the semileptonic $pp \to b'Z \to bZZ \to bjj\ell^+\ell^-$ channel, we assume that the leptonically decaying Z is fully reconstructed, and perform our analysis at the $bjjZ$ level. We multiply the cross section at the $bjjZ$ level by $\mathrm{BR}(Z \to \ell\ell)$. We could have indeed performed the analysis at the bZZ level, but because this channel will be limited by QCD background as we demonstrate below, we include the latter and perform the analysis at the $bjjZ$ level. We demand one tagged b-jet, and apply the following cuts: *Rapidity*: $-2.5 < y_{b,j,Z} < 2.5$, *Transverse momentum*: $p_{Tb,j,Z} > 0.1 M_{b_2}$, *Invariant-mass cuts*: $M_Z - 10\,\mathrm{GeV} < M_{jj} < M_Z + 10\,\mathrm{GeV}$, $0.95 M_{b_2} < M_{(bZ)\mathrm{OR}(bjj)} < 1.05 M_{b_2}$, where Z means the leptonically decaying Z, and in the last invariant-mass cut we accept the event if either of M_{bZ} OR M_{bjj} lies within the window. Here, j will exclude the b to avoid having to deal with combinatorics issues with the three bs that will be present if the Z decays to $b\bar{b}$. We ask that this not happen by demanding that the tagged-b is not among the two jets that reconstruct to the Z. We therefore multiply the signal $bjjZ$ and electroweak background $(bjjZ)_{EW}$ cross sections by $\eta_b \mathrm{BR}_{Z\to\ell\ell} = 0.033$ with $j = \{u, d, c, s\}$, where, we include the $Z \to b\bar{b}$ decays that fail the b-tag. Since experimentally light-quark jets and gluon jets cannot be differentiated effectively, for the background, we take $j = \{g, u, d, c, s\}$, and in addition to the bZZ SM background for which the multiplicative factor is as shown above, we include the QCD backgrounds, namely,

$$(bjjZ)_{\mathrm{QCD}} = (bjjZ) + (bjbZ)(1 - \eta_b) + (bbbZ)(1 - \eta_b)^2,$$

where a $(1 - \eta_b)$ factor is included for a b-quark that fails to be tagged, and, we multiply these with an overall multiplicative factor of $\eta_b \mathrm{BR}_{Z\to\ell\ell}$.

The signal and the background cross sections along with the luminosity required for the semileptonic decay mode for various values of $M_{b'}$ and κ given in Table I are shown in Table III. In the table, *primary cuts* includes all cuts except for the $M_{(bZ)\mathrm{OR}(bjj)}$ invariant-mass cut. The required luminosity for the semileptonic case is always background limited.

In Fig. 6 (right) we show the model-independent contours of the 14 TeV LHC luminosity required for 5σ significance with at least 10 signal events in the $\kappa_{b_2 bZ} - M_{b_2}$ plane. The region to the left of a contour is covered by that luminosity. $\mathrm{BR}(b' \to bZ) = 1/3$ is assumed. The kink seen is the crossover from being background limited at lower masses to signal rate limited at higher masses. The blue dots show the $M_{b'}$ and $\kappa_{b_2 bZ}$ given in Table I for which Table III applies.

Dileptonic decay mode: For the $pp \to b'Z \to bZZ \to b\ell^+\ell^-\ell^+\ell^-$, we perform the analysis at the bZZ level and multiply the cross section by $\eta_b * \mathrm{BR}(Z \to \ell\ell)^2$. We apply the following cuts: *Rapidity*: $-2.5 < y_{b,Z} < 2.5$, *Transverse momentum*: $p_{Tb,Z} > 25$ GeV, *Invariant-mass cut*: $0.95 M_{b_2} < M_{(bZ)} < 1.05 M_{b_2}$, where Z means either of the leptonically decaying Z, and in the invariant-mass

TABLE III. Signal and background cross sections at the 14 TeV LHC for the $pp \to b'Z \to bZZ \to bjjZ$ channel with its charge-conjugate process also included. The luminosity required in shown for the semileptonic decay modes corresponding to the benchmark masses and couplings shown in Table I. The $bjjZ$ columns neither include b-tagging factors nor BR($Z \to \ell\ell$), while $\mathcal{L}_{\text{SemiLep}}$ is shown after all these factors are included. $(bjjZ)_{\text{QCD}}$ shows the total QCD background computed using the different channels detailed in the second table weighted by appropriate factors as explained in the text.

$M_{b'}$ (GeV)	Signal σ_s (in fb) $bjjZ$		Background σ_b (in fb) $(bjjZ)_{EW}$		$(bjjZ)_{\text{QCD}}$		$\mathcal{L}_{\text{SemiLep}}$ (fb^{-1})
	Primary cuts	all cuts	Primary cuts	all cuts	Primary cuts	all cuts	
250	1017.66	995.86	77.03	10.33	7853.02	867.82	0.66
500	16.84	15.50	8.81	0.68	419.75	14.11	45.94
750	1.26	1.14	1.85	0.10	56.26	0.86	551.26
1000	0.14	0.12	0.47	0.01	12.38	0.05	3399.67

$M_{b'}$ (GeV)	QCD background (in fb)		
	$bjjZ$	$bjbZ$	$bbbZ$
250	546.36	634.32	17.19
500	10.14	7.76	0.35
750	0.52	0.66	0.03
1000	0.02	0.06	0.002

cut, M_{bZ} is evaluated for both the Zs with the event kept if either one of them falls within the window. We have relaxed the p_T cut here since we do not have to suppress the largish QCD background that we had to contend with in the semileptonic case. The signal and background cross sections along with the luminosity required for the dileptonic decay mode for various values of $M_{b'}$ and κ given in Table I are shown in Table IV. As before, in the table, *primary cuts* includes all cuts except for the $M_{(bZ)}$ invariant-mass cut. The required luminosity for the dileptonic case is always signal limited.

2. $bg \to b'Z \to tWZ$ channel

In this case, at the tWZ level, the three particles in the final state are different, and therefore there is no combinatorial issue. For the semileptonic decay mode we have two possibilities, namely, when the Z decays leptonically and the W hadronically, and vice versa. If the Z decays hadronically and the W leptonically, we have a neutrino in the final state, leading to missing momentum. At a hadron machine, since the incoming parton energies are not known, this missing momentum will prevent the full reconstruction of the event, but can only be done in the transverse plane. However, one can apply the W mass constraint in order to infer $p_{\nu z}$ (up to a twofold ambiguity) as explained, for example, in Ref. [24].

The signal and SM background at the tWZ level are shown in Table V. The choice for all the cuts here is similar to the ones for the dileptonic bZZ case above. Since the tW decay mode is present for a chiral b' also, and our main motivation in this study is to expose the vectorlike nature of the b', we have not computed the QCD background for this process, and have not determined the luminosity required.

3. $bg \to b'Z$, $b'h \to bZh$ channel

We assume a light Higgs with $h \to b\bar{b}$ (with BR ≈ 1), and the Z decaying leptonically, resulting in the $b\ell^+\ell^- b\bar{b}$ channel. We demand three b-tags. We perform the analysis at the bZh level and multiply the cross section by $\eta_b^3 * \text{BR}(Z \to \ell\ell)$, but for the QCD background which we take at the $bZb\bar{b}$ level (multiplied by effectively the same factor). The $bZb\bar{b}$ background is the same as in the

TABLE IV. Signal and background cross sections at the 14 TeV LHC for the $pp \to b'Z \to bZZ$ with its charge-conjugate process also included, and the luminosity required for the dileptonic decay mode corresponding to the benchmark masses and couplings shown in Table I. The bZZ columns neither include b-tagging factors nor BR($Z \to \ell\ell$), while $\mathcal{L}_{\text{DiLep}}$ includes all these factors.

$M_{b'}$ (GeV)	Signal σ_s (in fb) bZZ		Background σ_b (in fb) bZZ		$\mathcal{L}_{\text{DiLep}}$ (fb^{-1})
	Primary cuts	All cuts	Primary cuts	All cuts	
250	1119.42	1088.84	77	10.54	2.1
500	25.15	22.80	77	2.16	97.6
750	2.32	2.04	77	0.52	1091.9
1000	0.36	0.32	77	0.15	6962.4

TABLE V. Signal and background cross sections for the $pp \to b'Z \to tWZ$ channel with the charge-conjugate process also included. The κ are taken to be as given in Table I.

$M_{b'}$ (GeV)	Signal σ_s (in fb)		Background σ_b (in fb)	
	y, p_T cuts	All cuts	y, p_T cuts	All cuts
300	307.92	288.04	72.78	9.10
500	40.02	35.88	72.78	5.72
750	4.20	3.74	72.78	1.84
1000	0.70	0.62	72.78	0.64

TABLE VI. Signal and background cross sections for the leptonic $pp \to b'Z + b'h \to bZh$ channel. The bZh and $bbbZ$ columns neither include b-tagging factors nor BR($Z \to \ell\ell$), while $\mathcal{L}$ includes all these factors. The κ are taken to be as given in Table I.

$M_{b'}$ (GeV)	Signal σ_s (in fb)		Background σ_b (in fb)				$\mathcal{L}$ (fb^{-1})
	bZh		bZh		$bbbZ$		
	y, p_T cuts	All cuts	y, p_T cuts	All cuts	y, p_T cuts	All cuts	
250	1093.10	1056.96	4.68	0.74	569.35	18.01	1.13
500	44.30	34.70	4.68	0.14	569.35	2.22	34.41
750	5.94	3.54	4.68	0.03	569.35	0.37	337.30
1000	1.44	0.58	4.68	0.01	569.35	0.03	2058.67

previous case given in Table III. We show in Table VI the signal and background cross sections and the luminosity required. The luminosity is signal-rate limited.

We could perhaps gain in luminosity by only demanding one or two b-tags as opposed to the three we demand here, but then the QCD background may be too large. One could also consider the hadronic decay of the Z resulting in the $bbbjj$ channel, but the QCD background may be large. We have not considered these here.

C. Other processes

Here we collect some processes that we have considered, but have not analyzed in full detail, since based on rough estimates we think that they may lead to a larger luminosity requirement compared to the ones we have considered in detail above. We give below some indication for what cross sections we expect for these processes for the benchmark points given in Table I.

$bq \to b'q$ process: For the process $bq \to b'q$, the signal is induced by the t-channel exchange of a Z. We find the signal cross section to be small compared to the SM background. For example, for $M_{b_2} = 750$ GeV, the signal cross section for $bQ \to b'q \to bZq \to b\ell\ell q$ is about 0.65 fb, which is about 40 times smaller than the background, which we have computed with an invariant-mass cut of $|M_{bZ} - M_{b_2}| \leq 25$ GeV.

$bq \to qb'W$, $qb'Z$, $qb'h$ and $bg \to gb'Z$, $gb'h$ processes: The channels with a q in the final state proceed via bW and bZ fusion. The backgrounds are also bW and bZ initiated, and is potentially under control. But since the initial state is only q and b, this may not compare well to g initiated processes. The background is particularly small for $bq \to qb'Z \to qbhZ$ since h has to attach to b line which is suppressed by λ_b, the b-quark Yukawa coupling, and there is no ZZh coupling. Similar situation should also apply for the channel $bq \to qb'h \to qbhh$. Since experimentally we cannot tell the difference between a light q and g, we should include $bg \to gb'Z$, $gb'h$ here, which will result in the same final state as the above processes.

We expect these 3-body final state processes in general to have smaller cross section compared to the 2-body final states considered earlier. For $M_{b_2} = 750$ GeV and b' decaying as $b' \to bZ$ the total signal strength is about 0.08 fb (which includes the charge-conjugate process), with one of the Z decaying leptonically and the other decaying into light jets.

$qg \to qb'b$, $qb't$ processes: These proceed via gZ and gW fusion, respectively. Comparing to the $bg \to b'Z$ process, we see that this is a 3-body final state which would suppress the cross section.

For $b' \to bh$, the $qbhb$ irreducible background should be small since it is suppressed by λ_b^2. But, the SM background will include processes in which the q is replaced by a g, which will mean that the background is gg initiated, and is likely to be much larger.

$gg \to b'bZ$, $b'tW$, $b'bh$ processes: These processes are related to the $gg \to b'b'$, and being a 2-body process, it will be clearly bigger than the above 3-body processes if the $M_{bZ,tW,bh} = M_{b'}$ region is included. These channels will be important only if M_{b_2} is so large that phase-space considerations will favor this channel over on shell pair production.

$qq \to b'b$, $b't$ processes: The signal for the $b'b$ final state is small as this is a qq initiated process. For example, if we consider the b' decaying into a b and a Z with the Z decaying leptonically, the signal turns about 0.009 fb for

$M_{b_2} = 750$ GeV. Moreover, the background, which has gg initiated contributions, is expected to be much bigger than the signal.

$gg \to b'b$ and $gb \to b'g$ process: These proceed via s-channel and t-channel Higgs exchange, respectively, with an effective ggh vertex (top triangle diagram). We roughly estimate this contribution to be potentially bigger than the $\sigma(bg \to b'Z)$ we have considered earlier; however these channels are susceptible to the gg initiated SM background which is large, and therefore might lead to a larger required luminosity.

V. CONCLUSIONS

Many beyond the standard model extensions predict the existence of heavy vectorlike fermions. We consider the phenomenology of one such vectorlike fermion, called b', with electromagnetic charge $-1/3$ in a model-independent fashion. We write a general Lagrangian containing interactions of the b' with SM fields, identify the relevant parameters, namely, the b' mass, and, $b'bZ$, $b'tW$ and $b'bh$ couplings. We present analytical expressions for the b' partial widths to tW, bZ and bh final states.

Our main focus is the LHC signatures of a vectorlike b', the characteristic of which is the $\mathcal{O}(1)$ branching ratio into the bZ and bh decay modes in addition to the tW mode which is also present for a chiral (fourth generation) b'. Since our goal is to expose aspects unique to a vectorlike b' we consider the former two decay modes in detail.

We explore the $b'\bar{b}'$ pair production and, $b'Z$ and $b'h$ single-production processes at the 14 TeV LHC followed by their decays as mentioned above, namely, $b'\bar{b}' \to bZ\bar{b}Z$, $b'\bar{b}' \to bZ\bar{b}h$, $b'Z \to bZZ$ and $b'Z + b'h \to bZh$ channels. We list a few other b' single-production processes very briefly and mention the reasons why we do not consider them in detail. For the modes with two Zs, we consider the semileptonic decay mode where one Z decays hadronically and the other leptonically, and the dileptonic mode where both Zs decay leptonically, while, for the modes with a Higgs, we only consider the semileptonic mode where the Z decays leptonically and the Higgs into $b\bar{b}$ which is valid for a light Higgs.

We compute signal and background cross sections after pT, rapidity and invariant-mass cuts. As $M_{b'}$ goes from 250 GeV to 1 TeV, for the benchmark couplings shown in Table I, the $b'\bar{b}'$ pair-production signal cross section after our cuts ranges from about 68 pb to 28 fb, while the $b'Z + b'h$ single-production cross section ranges from about 1.4 pb to 0.4 fb. These are after including the corresponding charge-conjugate processes. We also show model-independent plots for how these cross sections vary as the $b'tW$, $b'bZ$, and $b'bh$ couplings and $M_{b'}$ vary. We identify the dominant SM backgrounds for the semileptonic and dileptonic decay modes, including the dijet QCD background for the semileptonic mode, in addition to the irreducible electroweak background. The dijet QCD background is substantial. For the $b'\bar{b}' \to bZbZ \to bjjb\ell^+\ell^-$ channel we find the LHC reach to be about $M_{b'} \approx 1250$ GeV with about 1300 fb^{-1}, while for the $b'Z + b'h \to bZh \to b\ell^+\ell^- b\bar{b}$ channel it is about $M_{b'} \approx 1000$ GeV with about 2050 fb^{-1}.

We thus highlight some channels that will be useful in establishing a b' state, and decay channels that reveal its vectorlike nature.

ACKNOWLEDGMENTS

We thank G. Moreau and R. Singh for discussions on related work at the "Physics at TeV Colliders" Les Houches 2009 workshop, P. Behera for discussions on b-tagging issues, and K. Agashe and T. Han for comments on the manuscript.

[1] L. Randall and R. Sundrum, Phys. Rev. Lett. **83**, 3370 (1999).
[2] J. M. Maldacena, Adv. Theor. Math. Phys. **2**, 231 (1998); Int. J. Theor. Phys. **38**, 1113 (1999).
[3] K. w. Choi and I. W. Kim, Phys. Rev. D **67**, 045005 (2003).
[4] K. Agashe, A. Delgado, M. J. May, and R. Sundrum, J. High Energy Phys. 08 (2003) 050.
[5] K. Agashe and G. Servant, J. Cosmol. Astropart. Phys. 02 (2005) 002.
[6] K. Agashe, G. Perez, and A. Soni, Phys. Rev. D **71**, 016002 (2005).
[7] C. Dennis, M. Karagoz Unel, G. Servant, and J. Tseng, arXiv:hep-ph/0701158.
[8] R. Contino and G. Servant, J. High Energy Phys. 06 (2008) 026.
[9] J. Mrazek and A. Wulzer, Phys. Rev. D **81**, 075006 (2010).
[10] J. A. Aguilar-Saavedra, J. High Energy Phys. 11 (2009) 030.
[11] M. Carena, A. D. Medina, B. Panes, N. R. Shah, and C. E. M. Wagner, Phys. Rev. D **77**, 076003 (2008).
[12] A. Atre, M. Carena, T. Han, and J. Santiago, Phys. Rev. D **79**, 054018 (2009); A. Atre, G. Azuelos, M. Carena, T. Han, E. Ozcan, J. Santiago, and G. Unel, J. High Energy Phys. 08 (2011) 080.
[13] S. Gopalakrishna, G. Moreau, R. K. Singh, in *Proceedings of the Les Houches Workshop on the Physics at TeV Colliders, 2009, Contribution 11*, edited by G. Brooijmans *et al.*, p. 129 (unpublished).
[14] S. Gopalakrishna, G. Moreau, R. K. Singh "Vectorlike b' in Warped Extradimensions" (unpublished).
[15] S. Gopalakrishna *et al.*, Pramana 76, 707 (2011), p. 719.

[16] T. Aaltonen *et al.* (CDF Collaboration), Phys. Rev. D **76**, 072006 (2007); Phys. Rev. Lett. **106**, 141803 (2011).
[17] P. Q. Hung and M. Sher, Phys. Rev. D **77**, 037302 (2008).
[18] S. Chatrchyan *et al.* (CMS Collaboration), Phys. Lett. B **701**, 204 (2011).
[19] K. Agashe, R. Contino, L. Da Rold, and A. Pomarol, Phys. Lett. B **641**, 62 (2006).
[20] J. Alwall *et al.*, J. High Energy Phys. 09 (2007) 028.
[21] A. Pukhov *et al.*, Report No. INP MSU 98-41/542; arXiv:hep-ph/9908288; A. Pukhov, arXiv:hep-ph/0412191.
[22] J. Pumplin, D. R. Stump, J. Huston, H. L. Lai, P. Nadolsky, and W. K. Tung, J. High Energy Phys. 07 (2002) 012.
[23] J. Kang, P. Langacker, and B. D. Nelson, Phys. Rev. D **77**, 035003 (2008).
[24] S. Gopalakrishna, T. Han, I. Lewis, Z. g. Si, and Y. F. Zhou, Phys. Rev. D **82**, 115020 (2010).